NASA-OAI

Collaborative Aerospace Research and Fellowship Program

at

NASA GLENN RESEARCH CENTER

2004

FINAL REPORT

OAI

Leveraging Resources Through Collaboration

NASA-OAI COLLABORATIVE AEROSPACE RESEARCH AND FELLOWSHIP PROGRAM

AT

NASA GLENN RESEARCH CENTER

AT LEWIS FIELD

CLEVELAND, OHIO

PREPARED BY THE CO-DIRECTORS:

ANN O. HEYWARD

VICE PRESIDENT, WORKFORCE ENHANCEMENT

OHIO AEROSPACE INSTITUTE

MARK D. KANKAM

UNIVERSITY AFFAIRS OFFICER

NASA GLENN RESEARCH CENTER

CONTENTS

INTRODUCTION

During the summer of 2004, a 10-week activity for university faculty entitled the NASA-OAI Collaborative Aerospace Research and Fellowship Program (CFP) was conducted at the NASA Glenn Research Center in collaboration with the Ohio Aerospace Institute (OAI). This is a companion program to the highly successful NASA Faculty Fellowship Program and its predecessor, the NASA-ASEE Summer Faculty Fellowship Program that operated for 38 years at Glenn. The objectives of CFP parallel those of its companion, viz.,

(1) to further the professional knowledge of qualified engineering and science faculty,
(2) to stimulate an exchange of ideas between teaching participants and employees of NASA,
(3) to enrich and refresh the research and teaching activities of participants' institutions, and
(4) to contribute to the research objectives of Glenn.

However, CFP, unlike the NASA program, permits faculty to be in residence for more than two summers and does not limit participation to United States citizens. Selected fellows spend 10 weeks at Glenn working on research problems in collaboration with NASA colleagues and participating in related activities of the NASA-ASEE program.

This year's program began officially on June 1, 2004 and continued through August 7, 2004. Several fellows had program dates that differed from the official dates because university schedules vary and because some of the summer research projects warranted a time extension beyond the 10 weeks for satisfactory completion of the work. The stipend paid to the fellows was $1200 per week and a relocation allowance of $1000 was paid to those living outside a 50-mile radius of the Center.

In post-program surveys from this and previous years, the faculty cited numerous instances where participation in the program has led to new courses, new research projects, new laboratory experiments, and grants from NASA to continue the work initiated during the summer. Many of the fellows mentioned amplifying material, both in undergraduate and graduate courses, on the basis of the summer's experience at Glenn. A number of 2004 fellows indicated that proposals to NASA will grow out of their summer research projects. In addition, some journal articles and NASA publications will result from this past summer's activities. Fellows from past summers continue to send reprints of articles that resulted from work initiated at Glenn.

This report is intended primarily to summarize the research activities comprising the 2004 CFP Program at Glenn.

RESEARCH SUMMARIES

Brief summaries of the fellows' research assignments follow. As is clear from the reports, some of the work is of sufficient importance and content to warrant reporting in the technical literature.

Name: **George Chatzimavroudis**
Education: Ph.D., Chemical Engineering
Georgia Institute of Technology

Permanent Position: Assistant Professor, Chemical & Biomedical Engineering
Cleveland State University

Host Organization: Microgravity Science Division
Colleague: 6728/Jerry G. Myers, Jr.

Assignment:

Development of an Imaging-Based, Computational Fluid Dynamics Tool to Assess Fluid Mechanics in Experimental Models that Simulate Blood Vessels

The hypothesis of this project is that image-based CFD is a realistic tool to reliably study complex fluid dynamics features in physiologic simulations of blood vessels. This particular Summer project will investigate the feasibility of this approach, by optimizing the imaging procedure that will enable the most precise reconstruction of the realistic geometry, which, in turn, will lead to accurate computations of the flow field. Therefore, the specific aims of this project are: (1) to determine the accuracy of image-based CFD in determining the blood flow dynamics characteristics in simulations of blood vessels; and (2) to determine the ability of CFD to predict changes in the flow field based on changes in the boundary conditions of the model. The following activities will be involved with this effort:

To achieve specific aim 1

1) Images from experimental models will be acquired in a 1.5 Tesla clinical MR scanner.
2) The cine-MR images will be used to reconstruct the 3D geometry. The vessel wall will be identified, segmented, and used to create the 3D geometry to be meshed.
3) After meshing, the CFD program will be executed and the computational solution for the 3D velocity will be compared with the MR velocity data.

In the microvascular approach:

4) Microvascular branching and flow will be visually imaged through the 2D optically accessible window of the quail embryo.
5) Using this approach as a template, a simulation of the quail vasculature will be initiated for CFD purposes.
6) Utilizing velocity fields obtained from micro-PIV analysis of the quail CAM, a similar approach will be taken, as on the vascular scale models, to investigate the reliability of the microvasculature CFD simulations.

To achieve specific aim 2

1) Images from the same experimental models as above will be acquired using the 1.5 Tesla MR scanner.
2) The MR images will be used to reconstruct the 3D geometry. The vessel wall will be identified, segmented and used to create the 3D geometry to be meshed.
3) After meshing, the CFD program will be executed and the computational solution for the 3D velocity will be compared with the MR velocity data.
4) Changes in the frequency of pulsation, will induce changes in the velocity profiles shown through the three-directional MR velocity measurements. In the CFD studies, frequency changes will be reflected in changes of the inlet flow waveform boundary condition.

It is anticipated that the results of this study will provide the first significant part of the required information for the construction of a realistic model of the cardiovascular system. In the context of the Digital Astronaut initiative, this study will begin to set the basis for the establishment of a technique to monitor and foresee changes in the cardiovascular system of astronauts during prolonged space missions.

Research Summary Submitted by Fellow:

Toward the Construction of the Digital Astronaut – Development of an Imaging-Based, Computational Fluid Dynamics Tool to Assess Fluid Mechanics in Experimental Models that Simulate Blood Vessels

INTRODUCTION

The <u>long-term goal</u> of this project is to develop a computational tool able to simulate the cardiovascular system (as part of the Digital Astronaut), both from the geometrical point-of-view, but also from the functional point-of-view. This means the development of a model that will be able to couple blood motion characteristics with vessel wall motion characteristics. The <u>hypothesis</u> of this project was that image-based CFD is a realistic tool to reliably study complex fluid dynamics features in physiologic simulations of blood vessels. This particular summer project investigated the feasibility of this approach, by studying the reliability of reconstruction of the realistic geometry (using image data), which, in turn, would lead to accurate computations of the flow field. The <u>aim</u> of this project was to determine the accuracy of image-based CFD in determining the blood flow dynamics characteristics in simulations of blood vessels.

The primary tool for achieving physiologically realistic geometries in this study was magnetic resonance (MR) imaging. MR imaging provides reliable anatomical and accurate dynamic flow blood information in the cardiovascular system. It is the only clinical technique able to measure all three spatial components of the velocity vector at any location. Therefore, MR offers an excellent tool for an initial pre-launch evaluation of the cardiovascular system of an astronaut. MR imaging provided the necessary information to reconstruct the cardiovascular geometry and the necessary flow boundary conditions in order to run the simulations.

METHODS

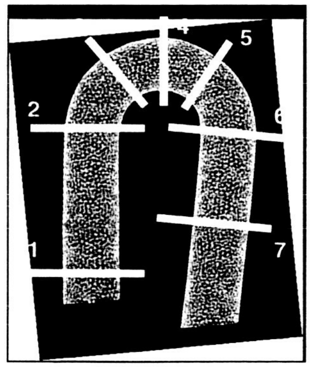

Figure 1: *Schematic of the model and placement of the imaging slices for the 3-DIR velocity-encoded MR acquisitions*

MR images from a non-planar glass U-shaped model (Fig.1) were acquired in a 1.5 Tesla clinical MR scanner. The model was placed in a steady flow loop, which was then inserted inside the scanner. Water was used as the working fluid. Two flow rates were studied: 1.7 and 3.0 L/min.

First, scout images were acquired to localize the test section. Then, gradient-echo acquisitions were performed using a number of contiguous slides placed perpendicular to the long axis of the model. In the first straight part of the model before the arch, the images were in the transverse orientation. In the arch, the images were oblique sagittal. In the last part of the model after the bend, the images were oblique transverse. The slice thickness used was 3 and 5 mm. The field of view was 256x256 mm^2. The matrix size was 256x256 and 512x512, resulting in in-plane resolutions of 1x1 and 0.5x0.5 mm^2. These images were used to reconstruct the geometry of the model and execute the simulations with the CFD software.

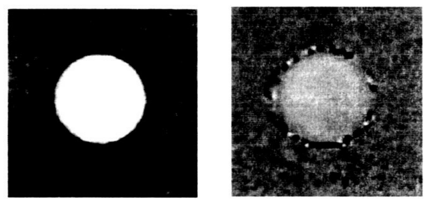

(a) (b)

Figure 2:
(a) Magnitude image reconstructed from the intensity of the received signal; (b) Phase (velocity) image reconstructed from the phase of the received signal which has the velocity encoded within it (linear relationship)

In order to have reference velocity data for the evaluation of the CFD results, three-directional (3-DIR) velocity-encoded MR acquisitions were performed using a gradient-echo sequence with velocity-encoding bipolar gradients in any of the three spatial directions. Fig.1 shows the seven axial acquisitions (perpendicular to the tube long axis locally). Two additional 3-DIR velocity acquisitions were performed along the horizontal centerline of the model. Since the model was non-planar, two acquisitions were necessary to image both straight parts.

<u>Analysis</u>: The MR images were used to reconstruct the 3D geometry as described in the following sections. In addition to the image-based geometry, an idealized geometry was constructed based on the model dimensions.

The contours of the edges (boundaries) of the vessel lumen were specified and saved in files containing the contour X,Y,Z coordinates. Then, they were used to create the geometry of the vessel. Finally, the geometry was saved in a file and became accessible for CFD. Unstructured tetrahedral meshes were generated for both the "MRI-generated" model and the "Idealized" model.

Each of the velocity-encoded MR acquisitions produced two images: a magnitude image and a phase image (Fig.2). The phase image contained the velocity information. Based on the data acquisition sequence used, the phase of the received signal is proportional to the velocity of the protons. The proportionality constant was known, therefore the velocity can be obtained.

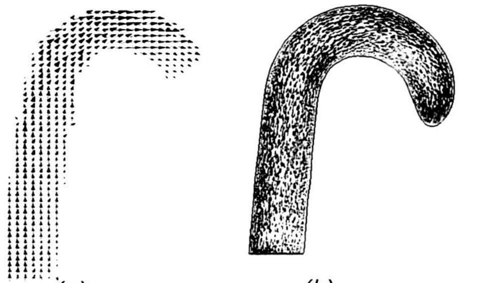

(a) (b)

Figure 3: *Vector-plot comparison between (a) the MR-measured and (b) the image-based-geometry CFD solved in-plane velocity patterns along the center-plane of the ascending straight part and the arch. A general agreement exists between the profiles*

The inlet flow rates as measured with MR were calculated from the through-plane velocity data at the inlet of the model (slice 1 in Fig.1). By summing the products "pixel velocity x pixel area" for all lumen pixels, the flow rate can be calculated.

Surface and contour plots were constructed from each velocity component of interest. Velocity vector plots were constructed by combining the two in-plane velocity components in a slice.

RESULTS

In general, both the surface/contour plots and the vector plots showed agreement in the velocity patterns between the MR and the CFD data (Fig. 3 and 4). Small (although quantitatively minor) differences were found between the "image-based" and the "idealized" geometry CFD results. The differences observed are due to small differences in the actual geometry of the models. This suggest that an idealized geometry may not always reproduce accurately the real flow field of a true blood vessel (especially when of interest are local features such as wall shear stresses, etc.). For both flow rates studied, the MR-measured values (at the inlet, slice 1) agreed very closely (difference <5%) with the calibrated rotameter readings.

CONCLUSION

This study illustrated, quantitatively, that reliable CFD simulations can be performed with MRI-reconstructed models and gives evidence that a future, subject-specific, computational evaluation of the cardiovascular system alteration during space travel is feasible.

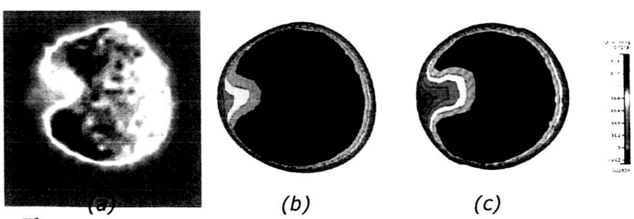

(a) (b) (c)

Figure 4:
Comparison between (a) the MR-measured, (b) the image-based-geometry CFD solved, and (c) the idealized-geometry CFD solved through-plane velocity profiles at the top of the arch (slice 4). Close agreement is seen between the three profiles (local differences <10%) with the stronger velocity activity at the outer tube side

Note:
This work was submitted to the 2005 SPIE Medical Imaging International Symposium

Name: **David G. Hehemann**
Education: Ph.D., Chemistry
Cleveland State University

Permanent Position: Scholar in Residence, Chemistry
Cleveland State University

Host Organization: Power and On-Board Propulsion Technology Division
Colleague: 5410/Aloysius F. Hepp

Assignment:

Analysis of Nanomaterials Produced from Precursors

This project will involve characterization of precursors and nanomaterials for photovolatic applications. Materials include II-VI and I-III-VI2, materials such as Zinc Oxide, Cadmium Sulfide, Copper Indium Diselenide and related materials. Equipment to be used will include characterization methods such as XRD, SEM, and a Precursor Analysis tool (GC, MS, FTIR, TGA) to establish the efficiency of nanoparticle production from chemical precursors. The fellow will be part of a research team that includes NASA and University researchers as well as students. Some involvement in the sysnthesis and growth of thin films and nanomaterials will also be required. It is expected that several publications will arise from this work and the fellow will be asked to assist in the writing of papers.

Research Summary Submitted by Fellow:

Organic Polymer Solar Cell Preparation

There is currently a great deal of interest in exploring the application of organic materials, such as conjugated polymers and small molecules, in electronic devices, for example, sensors, electroluminescent devices (LEDs), thin film transistors (TFTs), and photodiodes. Organic materials as the active components possess several advantages over their silicon counterparts, for example, ease of preparation, low processing cost, and a nearly unlimited variability. Fabrication of organic materials into solar cells or photodiodes is one of the most active areas among these investigations as appreciable photovoltaic effects such as, open-circuit voltages of 0.1-1.0 V, are easily obtained at moderate light intensity. Albeit, the relationship between material structure and critical device properties, for example, short-circuit current density (Jsc), open-circuit voltage (Voc), and carrier concentration, is still unclear in organic photocells. In organic materials, the intramolecular and intermolecular interactions differ greatly, with the latter being relatively weak van der Waals dispersion forces. The weak intermolecular forces allow for local structural disorder, and polymers may have amorphous and crystalline regions as well as chemical impurities.

Over the last decade, organic thin-film photovoltaic devices based on soluble conducting polymers have attracted a great deal of attention. The photovoltaic effect involves the generation of electron and hole pairs and their subsequent collection at opposite electrodes. In inorganic materials, the photon absorption produces free charge directly, while in organic materials, the photon absorption causes a delocalization of the excited states, which leads to a generation of bound electron–hole pair, "excitons". These excitons must dissociate into free charges in order to be transported to their respective electrodes. Exciton dissociation is known to occur in strong electric fields normally found at polymer–metal interfaces and at dissociation centers, such as oxygen impurities acting as electron traps. This feature has led several researchers to the idea of blending polymers with electron acceptor molecules, having a larger electron affinity than the polymer. Under these conditions, internal junctions between the polymer (electron donating and hole accepting) and the electron acceptor molecule (hole donating) are created. This allows the preferential transfer of the electrons into the electron acceptor molecule while leaving the holes to be preferentially transported through the polymer, a process known as photoinduced charge transfer.

We have been working on the preparation of a photochemical Schottky diode using organic polymers positioned between contacts having different work functions. The anodic contact consisted of a glass plate coated with Indium Tin Oxide, ITO. An organic conducting polymer, poly(3-octylthiophene), P3OT. The cathodic contact consisted of a painted on silver suspension. The polymer was spin coated onto the ITO coated glass plate. Spin coating was performed using a solution of the P3OT in toluene. Initial work dealt with how to prepare the spin coated polymer films. Dripping the solution onto the spinning slide led to a layer that exhibited a great deal of swirling and uneven thickness. It was found that the best method to prepare the polymer layer consisted of placing the polymer solution of the slide prior to spinning it. Then slowly spin the slide up to produce a uniform film. Using this method, it was found that uniform thin films of the polymer could be produced. Voltage and conductivity measurements of the system produced in this way showed that there was no diode effect produced in this system.

It was decided that perhaps the reason no diode effect was observed is that the cathodic contact had to high a work function to allow a high enough electric field to cause electron abstraction. To correct this situation we tried to use metal contacts that were more reactive. In particular, we went to an aluminum contact to try and prepare a measurable diode. We tried press fitting the contacts, gluing the contacts and finally evaporating the contacts onto the polymer film. In each case, no measurable photodiode effect was observed.

Next we felt that perhaps contact with atmospheric oxygen was oxidizing the polymer. To prevent this from happening, we placed the entire apparatus for preparing the diode in a controlled atmosphere unit filled with argon. The same series of preparations using both silver and aluminum as the cathodes were prepared again but this time under the inert atmosphere. Again voltage measurements using these cells showed no diode effect. Finally, we decided to try forming the polymer solutions using different solvents because the film morphology is affected by the solvent used in the film preparation. We are in the process of looking at chloroform and mixed toluene – tetrahydrofuran solvent systems to prepare the diode. Work is continuing in this area to prepare the diode to look further into the preparation of solar cells based on this polymer system.

Name: **Okechukwu Ugweje**
Education: Ph.D., Electrical Engineering
Florida Atlantic University

Permanent Position: Associate Professor, Electrical and Computer Engineering
The University of Akron

Host Organization: Communications Technology Division
Colleague: 5640/Roberto J. Acosta

Assignment:

LEO Propagation Analysis Tool

Future satellite communications systems operating in Ka-band frequency band are subject to degradation produced by the troposphere which is much more severe than those found at lower frequency bands. These impairments include signal absorption by rain, clouds and gases, and amplitude scintillation's arising from refractive index irregularities. This project will developed a tool to predict fade attenuation due to atmospheric impairments at Ka-band for low earth orbiting satellites links at Ka-band and above. This tool will be developed in MATLAB and will contain the latest ITU-R recommendations for attenuation predictions and will be integrated with STK orbit prediction tool.

Research Summary Submitted by Fellow:

Antenna Systems Engineering and Propagation Data Analysis

Abstract
This research is two fold. First is the antenna systems engineering for the proposed Lunar Mission was undertaken. Using a preliminary architecture of the lunar mission, the relevant antenna system parameters were calculated. This include the variation of G/T and EIRP given that the system margin is between 0 – 5 dB. From the calculations, the antenna size and power were determined for each link. The second component is the analysis of ACTS Ka-band experimental data using the White Sands, New Mexico data. In this case, we analyzed a five-year measured data and then determined the precision in which Ka-band antenna pattern measurement can be perform at this site. This task is in support of the solar dynamic observatory satellite system, which will operate on the 25.5 - 27 GHz band.

Summary of "Antenna Systems Engineering for the Lunar Mission"
The overall straw man's space communication link architecture for the Lunar Mission is shown in Fig. 1 [1]. This link is formulated based on information available at the time and information collected through other preliminary studies on Lunar Mission [2]. We

investigated the space architecture in an integrated fashion while addressing only the communication link requirements and parameters.

The communication links consist of a constellation of communication orbiters; high and low data rate ground terminals Lunar Lander and Rovers. The architecture is represented by three architectural elements and five levels of communication links. The architectural elements are the Earth, Lunar Surface and Orbiters while the five duplex levels of communication links are Earth-to-Surface, Earth-to-Orbit, Orbit (moon)-to-Surface (moon), Surface (moon)-to- surface (moon), and Orbit (moon)-to-Orbit (moon). Collectively, links within and between these elements represent segments of the pathways needed to achieve the end-to-end data-passing capability envisioned for the mission.

Using this link architecture and parameters defined in [1], we calculated the EIRP and G/T for all the links. Our calculations included for high and low data rate links and for all possible frequencies - allocated, and unallocated but possible frequencies. Sample results are shown below. Since different studies on the Lunar Mission are on-going, the architecture and parameters are still evolving. Our computations could be used as the baseline study.

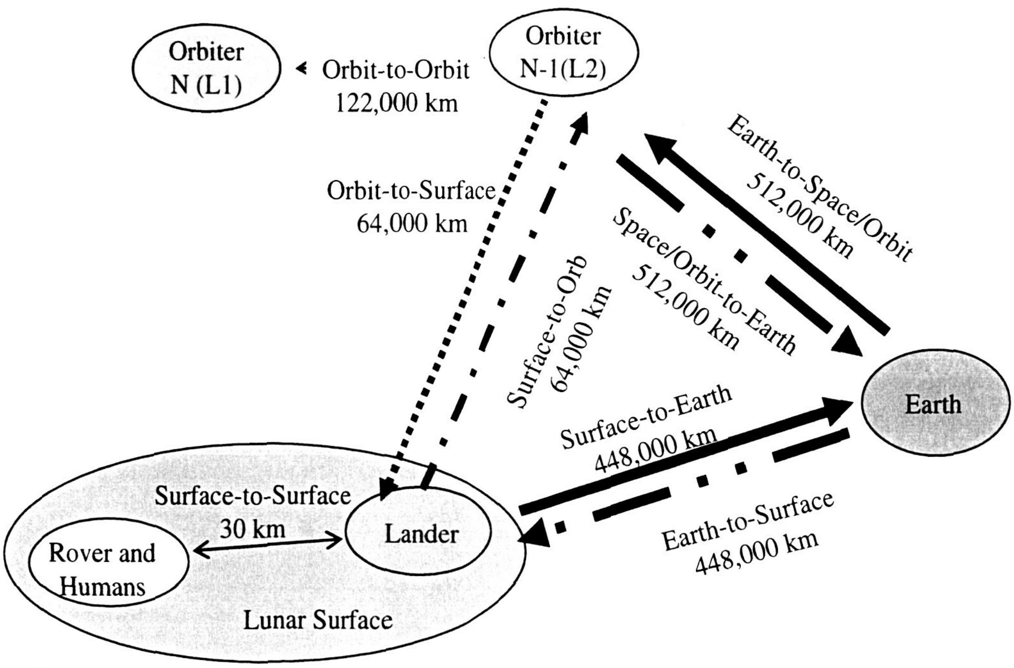

Figure 1: Integrated space communication architecture for the lunar mission.

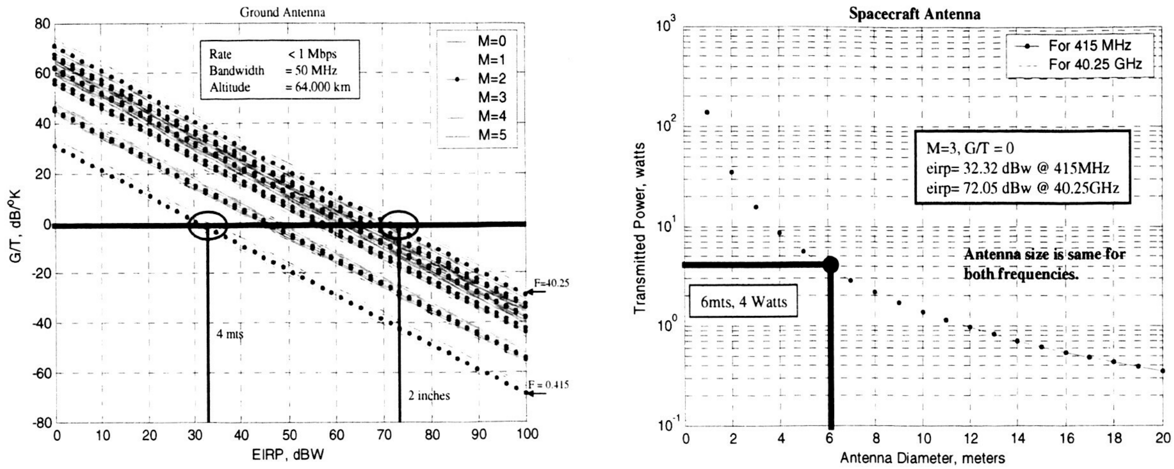

Figure 2: G/T vs. EIRP for Orbit-to-Surface link and the corresponding antenna size and power.

Summary of "Analysis of the 5-Year White Sands, New Mexico Propagation Data"

For this experiment, the data from ACTS propagation Terminal (APT) located at the Goddard White Sands Complex, New Mexico was used. Some antenna and system parameters are given in Figure 4. This terminal is one of seven identical propagation terminals used in the ACTS propagation campaign. The Attenuation relative to Free Space (AFS) or total attenuation was measured. AFS is a statistical distribution representing the attenuation due to all atmospheric propagation effects – gaseous absorption, clouds, scintillation, precipitation, etc. The data cover a 5-year period, January 1994 - December 1998, for two beacons at 20.2 GHz and 27.5 GHz.

The raw data were stored as a one-second sample value of attenuation. The one second measured attenuation data were sorted into 30 bins of size 1.0 dB between 0 and 30 dB. Our objective is to find the attenuation using the cumulative distribution function (CDF) method. Essentially by applying the formula:

$$C_n = \left(\sum_{k=n}^{N_{bin}} f_k / \sum_{k=1}^{N_{bin}} f_k \right) \times 100$$

where C_n is the percentage of time that attenuation exceeded the lower limit of the n-th intensity bin, f_k is the frequency of the k-th bin and N_{bin} is the total number of bins. Knowledge of the distribution of the attenuation is used to provide an adequate margin in a communication system.

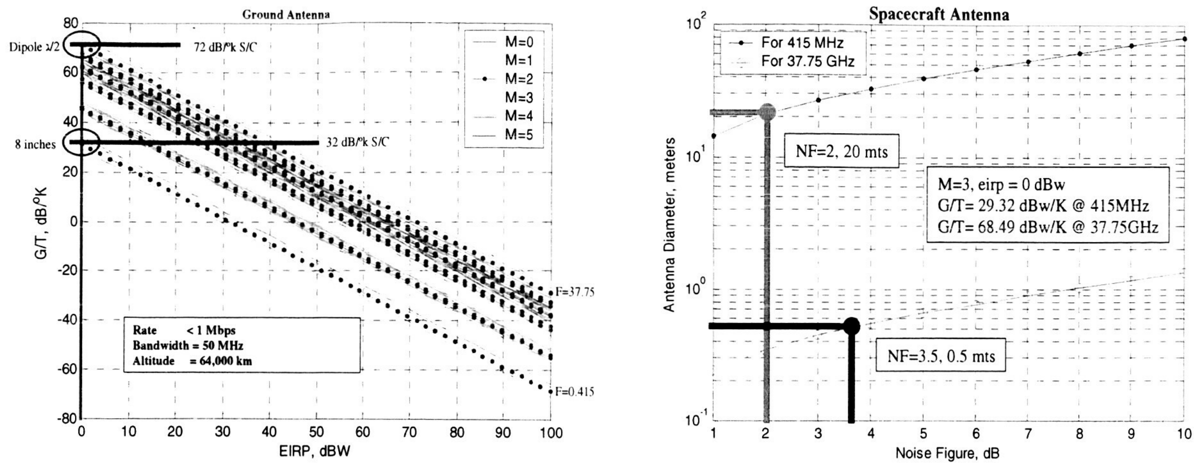

Figure 3: G/T vs. EIRP for Surface-to-Orbit link and the corresponding antenna size and power.

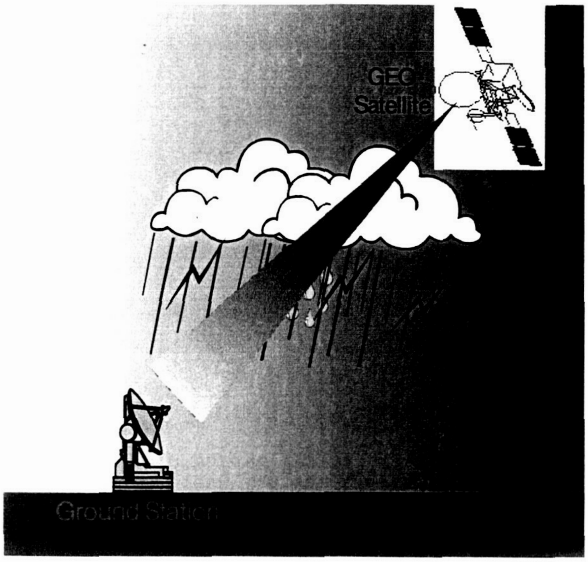

APT Parameters	
Terminal Location	Las Cruces, NM
Latitude	32°32'40"
Longitude	106°36'48"
Antenna Diameter	1.2 meters
Rain Region	Dry rain zone, ITU region M, Global Rain Region F
Elevation Angle	51 degrees
Azimuth	79 degrees
Satellite Location	100°W
Frequency (GHz)	20.2, 27.5 GHz
Beamwidth	0.85 degrees

Figure 4: Model and parameters of a typical ACTS propagation terminal.

For each year (1994 through 1998), we computed the monthly fade averages and fade spreads; the annual fade averages and fade spreads; determined the months with the best and worst fade statistics. For the 5-year period, we computed the monthly fade averages and fade spreads, as well as the average 5-year fade and spread. From these computations, we determined the required system margin.

Sample results are presented in Figures 5 and Table 1 shown below. The conclusion is that April (or March) is the best average month at 90 % availability with the smallest average fade at 0.43dB. This means that at this site, the antenna pattern can not be measured to a precision of less that about ½ dB for 52,560 minutes a year at best.

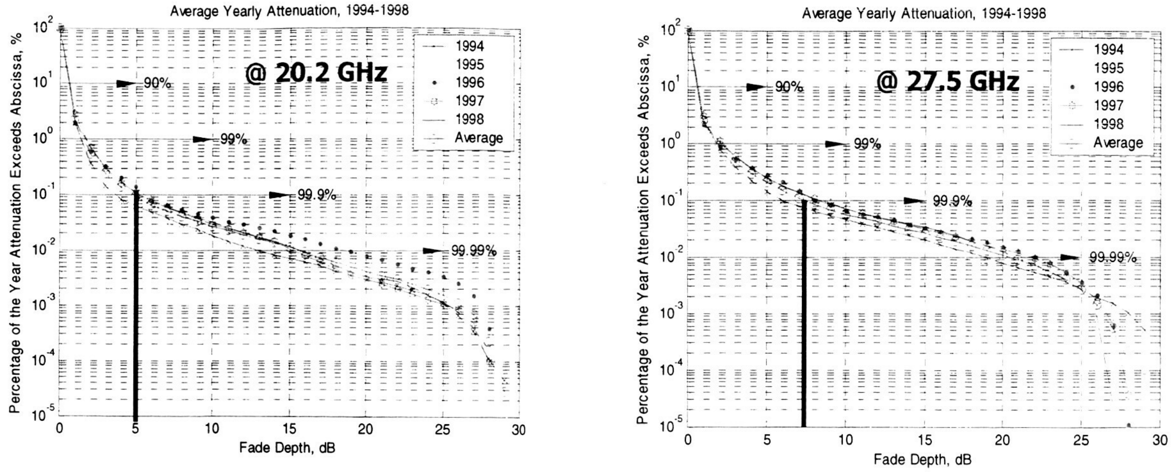

Figure 5: Average yearly attenuation @ 20.2 GHz and 27.5 GHz.

Table 1: Availability parameters for 5-year ACTS propagation Experiment

For 20.2 GHz			
% Availability	Best month	Worst month	Required Margin
90%	0.43	0.78/0.79	1.0 dB
99%	0.91	3.51	4.0 dB
99.9%	2.35	16.44	16.5 dB
99.99%	4.49	25.75	26.0 dB

For 27.5 GHz			
% Availability	Best month	Worst month	Required Margin
90%	0.42	0.78/0.79	1.0 dB
99%	0.84	2.47	3.0 dB
99.9%	1.75	13.35	15.5 dB
99.99%	3.27/3.30	25.35	25.5 dB

Other Task Completed:

Presentations:

1. "Antenna Systems Engineering and Propagation Data Analysis", Presented at the Brown Bag Seminar Series, Communications Technology Division, Thursday, August 5, 2004, @ Building 54, Room 101
2. "Antenna Systems Engineering and Propagation Data Analysis", presented at the NASA GRC Research and Technology Directorate, Insights in Research and Technology Lecture series, July 29, 2004, @ Ad. Bldg., Rm. 215

Panelist:

1. Served as a panelist on the NASA Glenn Research center Graduate Forum. Other panelist members are Drs. Hakimzadeh, Miranda, Johnson; and moderated by Dr. Kankam.

More Computations:

2. Develop a link equation MATLAB program analysis for propagation beacons. Analyze the GBS link for 180Kz band, 20Kz and 1 Hz

bandwidth. Report on the pointing to (Orbit and pointing angles descriptions) and link calculation on the GBS satellite.

Reference

[1]. Roberto Acosta, *et. al.*, “Antenna Systems Engineering – The Lunar Mission,” NASA GRC internal document, June 2004.
[2]. NASA, “The Vision for Space Exploration,” February 2004.